ation of the initially nondeprived eye had little, if any, effect in this animal (Table 1); however, its acuity had already risen to a value equal to that of the MD-DE animals deprived for the same duration. In this regard, it has been observed that the electrophysiological effects of reverse suture after the critical period are apparently variable between animals and that reverse suture is sometimes as effective as removing the nondeprived eye; however, the effects of reverse suture take longer to develop (*6*). Thus, the removal of the initially nondeprived eye in a reverse-sutured MD cat was sometimes, but not always, accompanied by a further increase in visual acuity. Whether or not this increase occurs may be determined by the final acuity reached after the reverse suture.

Combining all animals' visual acuity after enucleation, established after eight reversals in the staircase procedure with visual acuity measured in exactly the same way (*16*) after reverse suture, indicates that removing the nondeprived eye after the critical period was associated with higher final levels of a visual acuity than was reverse suture (Mann-Whitney U test, $U = 2$, $P = .048$ one-tailed test).

These results indicate that enucleation of the nondeprived eye in adult MD cats results in greater final visual acuity than does merely suturing closed the lids of the nondeprived eye. These behavioral results parallel increases in the percentage of responsive cells in the striate cortex of MD cats after enucleation (*4–6*) or reverse suture (*6*) of the nondeprived eye outside of the "critical period." The main differences between these recovery conditions is that the electrophysiological increase in the percentage of responsive cells seen after removal of the nondeprived eye is more rapid and usually greater (*6*). These same relationships were observed in the behavioral results of this study. These results are also in agreement with the effects of reverse suture or destruction of a portion of the central retina of the nondeprived eye in MD monkeys, in terms of both rate of acquisition and final acuity (*17*).

Experimentally induced monocular deprivation has been suggested as a model of human amblyopia (poor vision in one eye not due to refractive error or organic abnormality of the eye) (*18*). While comparisons from animal to human behavior must always be viewed cautiously, the correlation between the results of the present study and the literature in clinical ophthalmology further support the similarity between monocular deprivation in animals and human amblyopia. For example, in clinical treatment of human amblyopia, occlusion of the nonamblyopic eye is frequently used to improve vision using the amblyopic eye. This seems analogous to the effects of reverse suture in the MD cat and monkey. Moreover, it is a well-known but poorly documented finding (*19*) that some human amblyopes who suffer a loss of the nonamblyopic eye showed improved visual acuity through the amblyopic eye. This finding is also similar to my finding that removal of the nondeprived eye in an MD cat usually, but not always, results in improved visual acuity. Our knowledge of the neurophysiological correlates of these effects in the MD cat (*4–6*) may lead to a better understanding of the mechanism involved in human amblyopia and thus to improved techniques for correcting this disorder. Deprivation amblyopia in humans is the only condition that is directly analogous to monocular deprivation in animals; however, other types of amblyopia, while certainly different in cause, may be similar in terms of the effects on the brain.

DOUGLAS C. SMITH
Department of Psychology, Southern Illinois University, Carbondale 62901

References and Notes

1. D. Hubel and T. Wiesel, *J. Physiol. (London)* **160**, 106 (1962).
2. C. Blakemore and R. C. Van Sluyters, *ibid.* **237**, 195 (1974); D. Hubel and T. Wiesel, *ibid.* **206**, 419 (1970).
3. T. Wiesel and D. Hubel, *J. Neurophysiol.* **26**, 1003 (1963); *ibid.* **28**, 1029 (1965).
4. K. E. Kratz, P. D. Spear, D. C. Smith, *ibid.* **39**, 501 (1976).
5. P. D. Spear, A. Langsetmo, D. C. Smith, *ibid.* **43**, 559 (1980).
6. D. C. Smith, P. D. Spear, K. E. Kratz, *J. Comp. Neurol.* **178**, 313 (1978).
7. K. L. Chow and D. Stewart, *Exp. Neurol.* **34**, 409 (1972); P. Dews and T. Wiesel, *J. Physiol. (London)* **206**, 437 (1970); H. Hirsch and S. Tieman, *Brain Res.* **44**, 547 (1972); G. Rizzolatti and V. Tradardi, *Exp. Neurol.* **33**, 181 (1971).
8. K. P. Hoffman and M. Cynader, *Phil. Trans. R. Soc. London Ser. B* **278**, 411 (1977).
9. W. A. Harris and M. P. Stryker, *Soc. Neurosci. Abstr.* **3**, 562 (1977); D. P. Crewther, S. G. Crewther, J. D. Pettigrew, *J. Physiol. (London)* **282**, 181 (1978); R. C. Van Sluyters, *ibid.* **284**, 1 (1978).
10. U. C. Dräger, *J. Neurophysiol.* **41**, 28 (1978).
11. D. E. Mitchell, F. Giffin, F. Wilkinson, P. Anderson, M. Smith, *Vision Res.* **16**, 363 (1976).
12. D. C. Smith, *J. Comp. Neurol.*, in press; ———, R. Lorber, L. R. Stanford, M. S. Loop, *Brain Res.* **183**, 1 (1980).
13. All stimuli were 20 by 20 cm and held in black cardboard frames. For the luminance discrimination, the positive stimulus measured 156 cd/m^2, the negative 2.5 cd/m^2. For the stripe discrimination, the positive stimulus was a homogenous gray field with a luminance of 156 cd/m^2, and the negative stimulus was a 0.3 cycle/deg square-wave grating with a Michelson contrast of 99 percent and of the same average luminance. The square-wave gratings for establishing visual acuity went from 0.1 to 1.0 cycle/deg in 0.1 cycle/deg steps, from 1.0 to 3.0 cycle/deg in 0.25 cycle/deg steps and from 3.0 to 9.0 cycle/deg in 0.5 cycle/deg steps. Some of these square-wave gratings varied in luminance from the positive stimuli (all less than −18 cd/m^2). These variations were controlled by changing the luminance of the positive stimulus between 128 and 156 cd/m^2 from trial to trial. The phase of the stripe next to the cardboard frame was random.
14. T. N. Cornsweet, *Am. J. Psychol.* **75**, 485 (1962).
15. Eyes were refracted through the use of streak retinoscopy after the lids of the deprived eye were parted; none was found to be myopic. If anything, the deprived eye tended to be +1 to +2 diopters hyperopic.
16. S. Siegel, *Nonparametric Statistics for the Behavioral Sciences* (McGraw-Hill, New York, 1956). For this comparison the initial threshold acuity value obtained after reverse suture in RSE animals ($N = 3$) was used. Acuity of the enucleated animals includes that of all MD-DE animals and of the reverse-sutured cats after enucleation ($N = 6$).
17. A. Hendrickson, J. Boles, E. B. McLean, *Invest. Ophthalmol.* **16**, 469 (1977); J. Boles, J. R. Wilson, A. Hendrickson, *Soc. Neurosci. Abstr.* **4**, 620 (1978).
18. S. Awaya, Y. Miyake, Y. Imaizumi, Y. Shiose, T. Kanda, E. Komuro, *Jpn. J. Ophthalmol.* **17**, 69 (1973); H. M. Eggers and C. Blakemore, *Science* **201**, 264 (1978); G. K. von Noorden, *Invest. Ophthalmol.* **12**, 721 (1973).
19. H. M. Burian, *Am. J. Ophthalmol.* **1**, 1 (1969).
20. I thank M. S. Loop, A. Kirk, L. R. Stanford, and B. Holdefer for assistance in testing these animals, and A. Sorkin for performing the refractions. Portions of this work were completed while the author was supported as a postdoctoral fellow at the University of Illinois on training grant EYO 7005. This work was also supported by grant NSF BNS 8002251 and a research general grant 2-10396 from Southern Illinois University.

6 April 1981

Retinal Ganglion Cell Classes in the Old World Monkey: Morphology and Central Projections

Abstract. *Labeled ganglion cells were studied in whole-mount retinas of Old World monkeys after electrophoretic injections of horseradish peroxidase into physiologically characterized sites. A number of different morphological classes have been identified, each of which has a distinctive pattern of central projection. Since different functional classes of primate retinal ganglion cells also have distinctive patterns of central projection, correspondences between functional and morphological cell types have been inferred. There prove to be parallels between morphological types of cat and monkey ganglion cells.*

In both the cat (*1–8*) and the monkey (*9–12*), different functional classes of retinal ganglion cells have different patterns of central projection. A number of morphological classes of ganglion cells have also been described in both species (*13–17*), but much less is known of their central projections. Recently, a number of studies have described the sizes of the cell bodies of ganglion cells labeled by

0036-8075/81/0904-1139$01.00/0

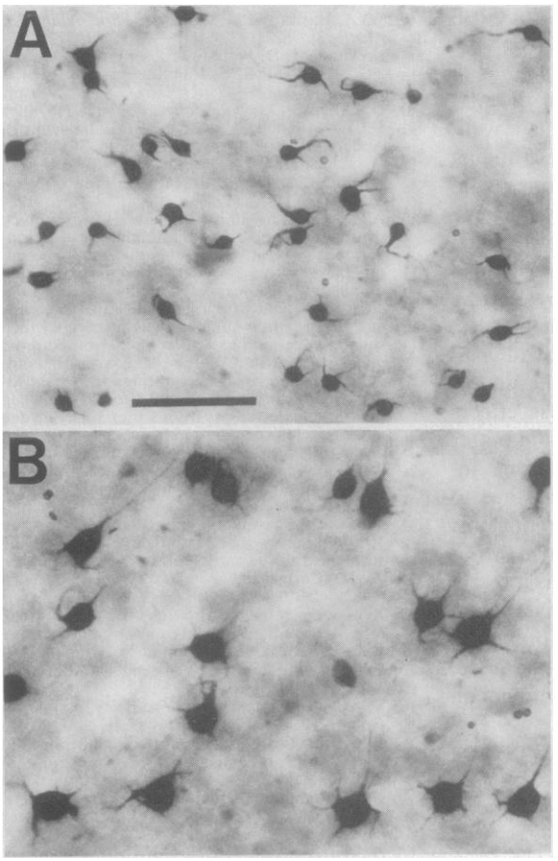

Fig. 1. Retrogradely labeled monkey retinal ganglion cells in neighboring regions in the same retina differing only in elevation. (A) B cells approximately 10 mm from the foveal slope, labeled by an electrophoretic injection of HRP into the parvocellular laminae of the LGN. (B) A cells approximately 10 mm from the foveal slope, labeled by an electrophoretic injection of HRP centered in magnocellular lamina 1 of the LGN. The positions of the receptive fields of the units recorded at the two injection sites allowed the patches to be differentiated unambiguously. Scale bar for both (A) and (B), 100 μm.

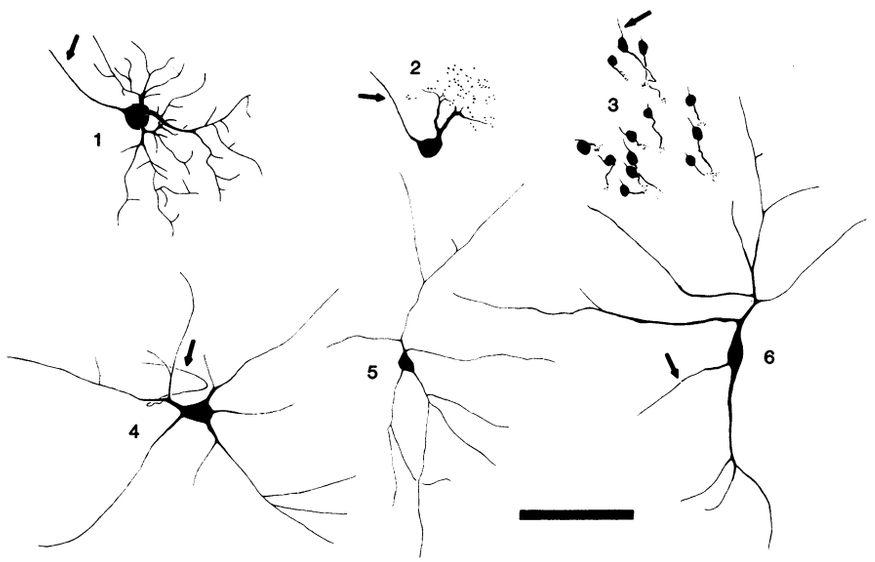

Fig. 2. Camera lucida drawings of ganglion cells belonging to the different morphological classes in the monkey retina. Very fine dendrites in our material were often visible as a series of HRP granules. These have been represented by continuous lines in the drawings only if continuity could be determined unambiguously. Scale bar, 100 μm. (Cell 1) An A-type cell, 6 mm from the fovea, labeled by an injection into the magnocellular laminae of the LGN; A cells were also labeled by injections into the superior colliculus and pretectum. (Cell 2) B cell, 7 mm from the fovea, labeled by an injection into the parvocellular laminae of the LGN; B cells were observed only after injections into the parvocellular laminae. (Cell 3) Cluster of B cells on the foveal slope, labeled by an injection into the parvocellular laminae. (Cell 4) E cell, 6 mm from the fovea, labeled by an injection into the pretectum. (Cell 5) C cell, 3 mm from the fovea, labeled by an injection into the pretectum; C cells were also observed after injections into the superior colliculus. (Cell 6) An unclassified cell 6 mm from the fovea, labeled by an injection into the pretectum.

injections of horseradish peroxidase (HRP) into central visual regions (*18–21*). These studies suggest that different morphological classes have distinct patterns of central projection.

Our aims were to identify the morphological classes of ganglion cells projecting to different visual regions in the Old World monkey (*Macaca fascicularis*) and to compare these classes and their projections with those in the cat. We electrophoretically injected HRP through microcapillary electrodes into physiologically characterized brain sites (*22*). The effective uptake sites resulting from such injections can be as small as a few hundred micrometers in diameter and can thus be localized within any area receiving retinal afferents. After an appropriate survival time, the animals were perfused; a procedure based on the *p*-phenylenediamine-pyrocatechol reagent and cobalt intensification (*23*) then permitted visualization of HRP reaction product in the axons, dendrites, and cell bodies of the retrogradely labeled ganglion cells (Figs. 1 and 2).

In the monkey, we have found a number of different morphological classes of retinal ganglion cells, which we have termed A, B, C, and E (Fig. 2, cells 1 to 5). Some ganglion cells that do not fit clearly into these classes were also found (Fig. 2, cell 6) (*24*).

The A cells have large cell bodies and medium-sized, characteristic dendritic fields (*25*) (Fig. 1B; Fig. 2, cell 1; Fig. 3). They have the coarsest axons of any ganglion cell type in the monkey retina (Fig. 4) (*26*). It is unlikely that there is a strict relationship between A cells and any of Polyak's morphological classes.

The B cells have small cell bodies (Fig. 1A; Fig. 2, cells 2 and 3) and fine to medium axons (Fig. 4). They have the smallest dendritic fields of any of the ganglion cell types in the monkey retina (Fig. 3). Near the fovea most have one principal dendrite that terminates in a characteristic, stratified (*14*) treetop (Fig. 2, cell 3). In the periphery, these cells have larger cell bodies and two or three main dendrites, and their dendritic fields are larger (Fig. 2, cell 2; Fig. 3A). It is unlikely that there is a strict relationship between B cells and any of Polyak's classes, although B cells in central retina do fit Polyak's description of midget ganglion cells.

The C cells have small cell bodies, fine axons, and very large dendritic fields (Fig. 2, cell 5; Figs. 3A and 4). The C cells within 3 mm of the fovea often have dendritic fields larger than those of A cells in the far periphery (Fig. 2, cell 5).

These cells remind us of the small diffuse ganglion cells of Polyak (*13*).

The E cells have medium to large cell bodies, fine to medium gauge axons and very large, distinctive dendritic fields (Fig. 2, cell 4; Figs. 3A and 4). This type of cell, which does not seem to have been described or drawn by Polyak, resembles cat ϵ cells (*16*).

Some cells in our sample did not fit clearly into any of the four classes. We do not yet know whether these cells represent distinct classes, subtypes of the groups already described, or simply unusual examples of familiar types. Some of these resemble the cells Polyak termed garland cells and have small to medium cell bodies, fine axons, and large dendritic fields consisting of fine dendrites that branch more than those of C cells. Others share a number of characteristics with E cells. These cells have cell body, dendritic field, and axon diameters within the E cell range. Nevertheless, the morphology of these cells differs from that of typical E cells (Fig. 2, cell 6).

The sizes and morphologies of A and B cells vary gradually with distance from the fovea. Changes include increases in cell body diameter, dendritic field diameter, and number and gauge of principal dendrites (Fig. 3).

After the injections of HRP into the parvocellular laminae of the lateral geniculate nucleus (LGN), all of the cells that stained well enough to be classified were B cells (Fig. 1A). In contrast, all classifiable cells resulting from injections into the magnocellular laminae were A cells (Fig. 1B). However, a few lightly labeled cells with small cell bodies were seen after an injection centered in magnocellular lamina 1 of the LGN. These cells were not labeled well enough to be definitively characterized, but they could represent a projection from small cells to the ventral S laminae.

Injections into the superior colliculus labeled A cells, C cells, and some cells that remain unclassified. Finally, injections into the pretectum labeled A cells, C cells, E cells, and some unclassified cells.

Bunt *et al.* (*21*) injected HRP into the monkey LGN and superior colliculus and reported that all retinal ganglion cells project to the parvocellular laminae of the LGN. In contrast, none of our injections into the parvocellular laminae labeled all retinal ganglion cells in any region of the retina. In particular, no A, C, or E cells were labeled by injections into these laminae. In all regions of the retina, however, the spatial density of cells labeled after injections into the parvocellular laminae was greater than that after other injections, presumably reflecting a high proportion of B cells in the monkey retina. In agreement with Bunt *et al.* (*21*), we have found that large cells (A cells) project to the magnocellular laminae, and cells of different sizes (A cells, C cells, and unclassified cells) project to the superior colliculus.

In the monkey, A cells project to the magnocellular laminae, which reportedly contain only relay cells with Y-like properties; B cells project to the parvocellular laminae, which reportedly contain only relay cells with X-like properties (*10–12*). Thus, A and B cells presumably have Y-like and X-like properties, respectively. Other receptive field types, which project to the pretectum and superior colliculus (*11*), are therefore likely to correspond to the remaining morphological types which project to these regions.

The physiological class of cells in the parvocellular laminae of the monkey LGN that has been termed X-like (*10*) actually includes a number of receptive-field types (*9–11*); each of these may have a distinctive morphology. Although all B cells labeled by injections into the parvocellular laminae share a number of properties, the dendritic branching patterns of adjacent B cells can differ, suggesting diversity within this class.

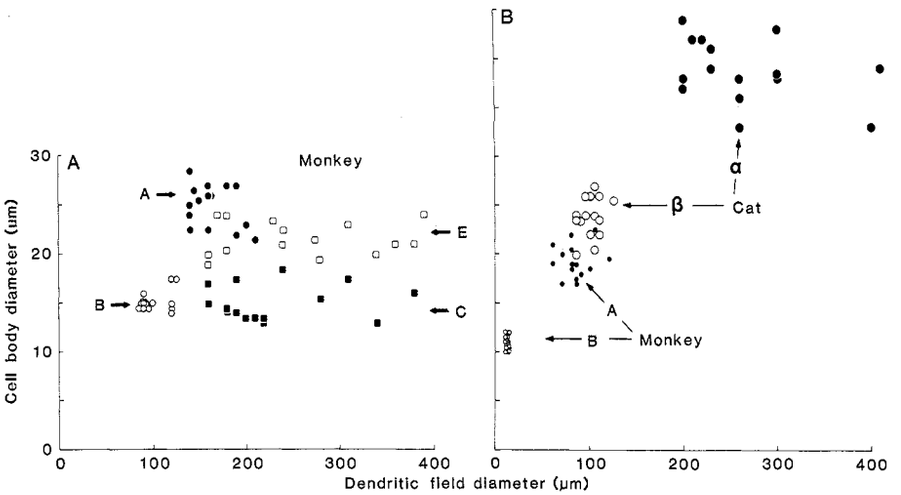

Fig. 3. Cell body and dendritic field diameters of cells belonging to the different morphological classes of monkey and cat retinal ganglion cells. Identical procedures were used in experiments on cats and monkeys. (A) All cells were 10 to 12 mm from the fovea. (B) α and β cells in the cat retina 2 to 4 mm from the area centralis and A and B cells in the monkey retina 2 to 4 mm from the foveal slope.

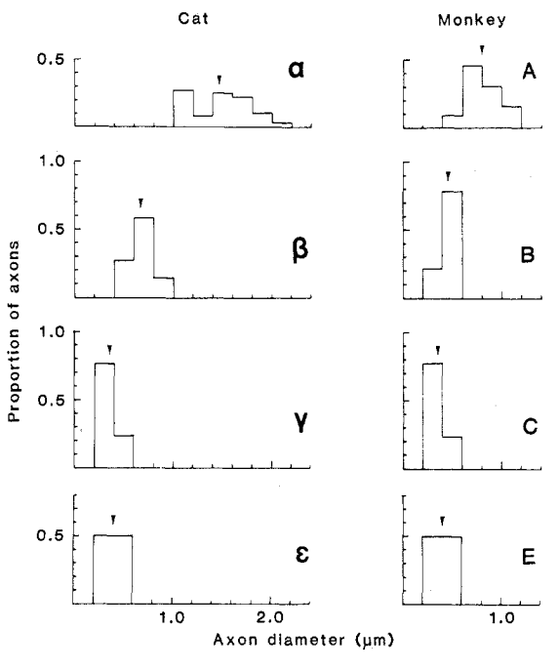

Fig. 4. Axon diameters of cells belonging to the different morphological classes of retinal ganglion cells in cat and monkey. All cells were more than 5 mm from the central area. Sample sizes for histograms: α, 54; β, 89; γ, 21; ϵ, 14; A, 33; B, 42; C, 30; and E, 12. The mean axon diameter for each histogram is indicated by an arrow.

Although A and B cells in the monkey differ morphologically from α cells and β cells in the cat, the relative differences between monkey A and B cells in their central projections, somal size, dendritic field size, and axon caliber are, for the most part, qualitatively similar to the corresponding differences between cat α and β cells. Thus, in cats and monkeys, just as there are parallels between different ganglion cell types in their functional properties, there seem to be parallels in their structural properties and central projections. As in the cat and other mammals, visual function in primates seems to be mediated by a variety of different classes of retinal ganglion cells that have distinctive patterns of central projection.

AUDIE G. LEVENTHAL
Department of Anatomy, University of Utah College of Medicine, Salt Lake City 84132
R. W. RODIECK
Department of Ophthalmology, University of Washington, Seattle 98195
B. DREHER
Department of Anatomy, University of Sydney, Sydney, New South Wales 2006, Australia

References and Notes

1. Y. Fukada and H. Saito, *Tohoku J. Exp. Med.* **106**, 209 (1972).
2. B. G. Cleland, M. Dubin, W. R. Levick, *J. Physiol. (London)* **217**, 473 (1971).
3. K.-P. Hoffman, J. Stone, S. M. Sherman, *J. Neurophysiol.* **35**, 518 (1972).
4. K.-P. Hoffman, *ibid.* **36**, 409 (1973).
5. B. G. Cleland and W. R. Levick, *J. Physiol. (London)* **240**, 421 and 457 (1974).
6. Y. Fukada and J. Stone, *J. Neurophysiol.* **37**, 749 (1974).
7. B. G. Cleland, W. R. Levick, R. Morstyn, H. G. Wagner, *J. Physiol. (London)* **255**, 299 (1976).
8. P. D. Wilson, M. H. Rowe, J. Stone, *J. Neurophysiol.* **39**, 1193 (1976).
9. T. N. Wiesel and D. H. Hubel, *ibid.* **29**, 1115 (1966).
10. B. Dreher, Y. Fukada, R. W. Rodieck, *J. Physiol. (London)* **258**, 433 (1976).
11. P. H. Schiller and J. G. Malpeli, *J. Neurophysiol.* **40**, 428 (1977); *ibid.* **41**, 788 (1978).
12. S. M. Sherman, J. R. Wilson, J. H. Kaas, S. V. Webb, *Science* **192**, 475 (1976).
13. S. L. Polyak, *The Retina* (Univ. of Chicago Press, Chicago, 1941).
14. B. B. Boycott and J. E. Dowling, *Philos. Trans. R. Soc. B* **255**, 109 (1969).
15. B. B. Boycott and H. Wässle, *J. Physiol. (London)* **240**, 397 (1974).
16. A. G. Leventhal, J. Keens, I. Törk, *J. Comp. Neurol.* **194**, 535 (1980).
17. J. Stone and R. Clarke, *ibid.* **192**, 211 (1980).
18. J. P. Kelly and C. D. Gilbert, *ibid.* **163**, 65 (1975).
19. H. H. Magalhães-Castro, L. A. Murata, B. Magalhães-Castro, *Exp. Brain Res.* **25**, 541 (1976).
20. H. Wässle and R.-B. Illing, *J. Comp. Neurol.* **190**, 333 (1980).
21. A. H. Bunt, A. E. Hendrickson, J. S. Lund, R. D. Lund, A. F. Fuchs, *ibid.* **164**, 265 (1975).
22. A. M. Grabiel and M. Devor, *Brain Res.* **68**, 167 (1974); A. G. Leventhal, *Exp. Brain. Res.* **37**, 349 (1979).
23. More complete descriptions of the procedures used for the preparation, electrophysiological recording, electrophoretic injection, injection site reconstruction, and histochemistry are given elsewhere (*16*).
24. This study differs from previous ones in that retinal ganglion cells were stained with HRP, whereas others have studied ganglion cell morphology in Golgi material. It is possible that some fine detail evident in Golgi-stained material may not be equally visible in our material. Nevertheless, the cell bodies of the HRP-filled cells in our sample from the cat appear similar in size to those of cells impregnated with the Golgi-rapid technique and somewhat larger than cells impregnated with Golgi-Cox (*15*). The diameters of dendritic fields of cells in our cat material are similar to those obtained by Boycott and Wässle (*15*) with the Golgi-Cox technique. In relative terms, our measurements of axon gauge in cat are also consistent with Boycott and Wässle's description, although they did not attempt to quantify axon diameter. Thus, it is unlikely that the most completely stained cells we have observed appear significantly different from the Golgi-stained cells observed by others.
25. The cell bodies and dendritic fields of filled cells were measured under the microscope through the use of a calibrated eyepiece graticule and a ×50 or ×100 oil immersion objective (*16*).
26. Axons were measured under the microscope, through the use of a calibrated eyepiece graticule and a ×100 oil immersion objective. Measurements were made distal to the axon hillock at a point past the axon's initial taper. In order to estimate the accuracy of our measurements, a sample of axons was measured independently by each of us and any discrepancies noted. Differences were rarely > 0.2 μm.
27. Supported by NIH grants EY-02923, EY-03427, EY-05212, and EY-91730 and by the E. K. Bishop Foundation. R.W.R. is a Research to Prevent Blindness–James S. Adams scholar. We would like to thank B. B. Boycott, A. H. Bunt, A. E. Hendrickson, and H. Kolb for their comments on the manuscript.

3 February 1981; revised 18 May 1981

Behavioral Effects of Lead and *Toxocara canis* in Mice

Abstract. *Adult mice were administered the common parasite* Toxocara canis *or lead or both. The parasite clearly altered mouse performance on tests of exploration, activity, learning, and motor coordination; behavioral effects in mice receiving lead alone were less general. Consequences of* Toxocara *administration appeared attenuated in animals receiving both agents. Parasite larvae were found in the central nervous system in all infected mice.*

Although an estimated 500 million to 1 billion people are infected with parasites, the behavioral consequences of such infection are virtually unknown. One common parasite is *Toxocara canis*, the dog roundworm; its eggs are passed by the dog's feces and may remain viable in the environment for years. This parasite is carried by perhaps two thirds of all domestic dogs and is the primary agent of visceral larva migrans (VLM) in the United States (*1, 2*). In VLM, the ingestion of embryonated parasite eggs by abnormal hosts such as humans or mice results in second-stage larvae migrating through the visceral organs, where they can remain viable for years (*3*). The difficulty of diagnosing and treating VLM in humans emphasizes the need for additional information concerning its behavioral consequences.

Ingestion of lead, another environmental hazard, may result in profound toxic manifestations as well as more sub-

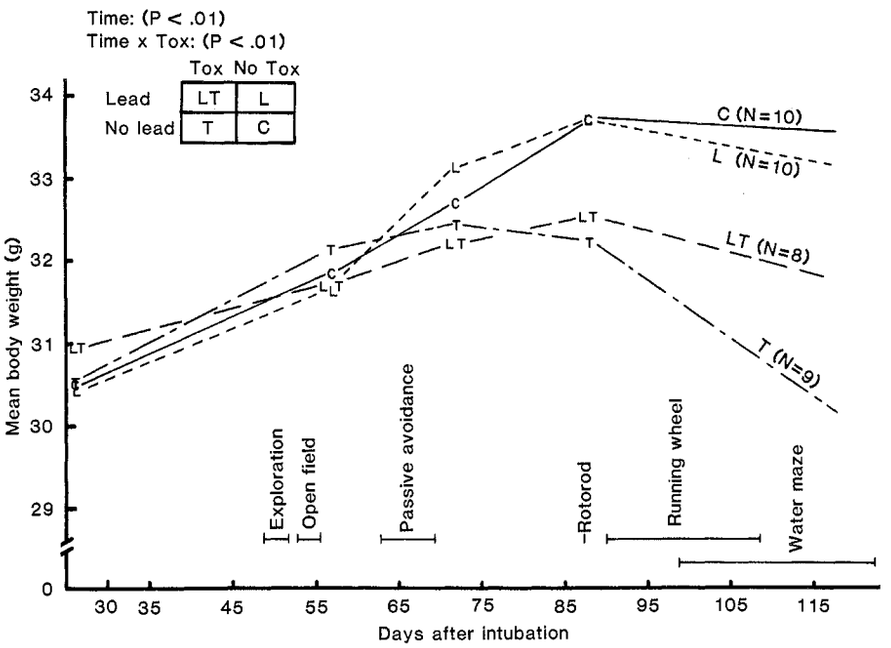

Fig. 1. Time line of body weight and behavioral measures. The four groups are represented by a 2 × 2 factorial design (inset). Results of analyses of variance with time as a repeated measure are presented in the upper left corner. All groups started with ten animals; *N* values give the number of animals surviving at the end of the experiment. *C*, control; *L*, lead; *T*, *Toxocara*; and LT, lead and *Toxocara*.

0036-8075/81/0904-1142S01.00/0